

A cable-scale experiment to explore new materials for optimizing superconductor accelerator magnets

C.J. Kovacs^{a,*}, E.Z. Barzi^b, D. Turrioni^b, A.V. Zlobin^b, M. Marchevsky^c

^a Center for Superconducting & Magnetic Materials (CSMM), Department of Materials Science & Engineering, The Ohio State University, USA

^b Applied Physics and Superconductivity Technology Division (APS-TD), Fermi National Accelerator Laboratory, USA

^c Applied Technology and Applied Physics Division (ATAP), Lawrence Berkeley National Laboratory, USA

ABSTRACT

A previously commissioned system for exploring critical current pressure sensitivity in superconducting cables, the Transverse Pressure Insert, was modified to examine signals resulting from strand motion and insulation/impregnation cracking in a fully-excited Nb₃Sn single strand embedded in an insulation wrapped and impregnated Cu dummy Rutherford cable stack. Measurements were performed in LHe with cyclic transverse pressures up to 68.5 MPa and transverse applied fields up to 13 T. Pressure was applied and removed to simulate stresses seen during magnet operation. Voltage and acoustic signal traces from a CTD-101 K impregnated cable stack were compared to those of a sample impregnated with NHMFL Mix-61. The experiments in this document were in the pursuit of developing a smaller scale, lower cost, and shorter turn around time experiment for exploring materials and processes to decrease training in next-generation Nb₃Sn accelerator magnets.

1. Introduction

High B_{irr} High Temperature Superconductors (HTS) composites would single handedly maximize peak magnetic field in the next-generation of accelerator magnets. However, conductor costs have led many to pursue developing a hybrid magnet consisting of a Low Temperature Superconductor (LTS) outer magnet [1]. For the high energy upgrade of the Large Hadron Collider (LHC) the proposed main bending dipoles have a Nb₃Sn outer magnet, a challenging task due to the performance requirements of the conductor and the large stresses within the magnet structure [2,3,4]. The large internal stresses during operation generate irreversible cracking and delamination of the magnet scale composite, and these mechanical disturbances are sufficient to generate quench due to low thermal margin of Nb₃Sn conductors [2]. Once a quench occurs, and the magnet safely recovers, it is necessary to excite the magnet again to the next higher level of internal stresses and mechanical disturbances. For Nb₃Sn, a significant number of these magnet ramping cycles are required to reach maximum field design specifications. So called “magnet training” results in significant time and costs in commissioning Nb₃Sn high field accelerator magnets.

There are multiple approaches for the reducing the number of training cycles [2,3,5], one of which is a material investigation for higher fracture toughness, better impregnating, and closer thermal expansion matching impregnant. To date, investigations of magnet training have only been performed once a Nb₃Sn magnet has been constructed. The sources of training in these prototype magnets can be

detected via acoustic detection, antennas, and voltage taps [6,7]. Demonstrated in this document is an exploratory sub-scale measurement to produce data relevant for Nb₃Sn accelerator magnet design. This sub-scale measurement will reduce the cost, complexity, and time necessary for investigating new materials and processes for magnet scale composites.

2. Methods

The Transverse Pressure Insert (TPI) in association with the Fermilab Teslatron II measurement station were chosen to perform these experiments, the TPI is shown in Fig. 1 [8]. Fig. 2.

2.1. TPI sample fabrication: pre-reaction assembly

The TPI samples consist of two 56.25 mm high electrical conductivity Cu Rutherford cable “blanks”, these blanks are from a dummy Rutherford cable and contain no superconductor, see Fig. 1. The ends of these cut blanks were welded to prevent spaying. A single Cu strand was carefully removed from one of the blanks and, after filing grooves into the welded ends of both blanks, replaced with a long length of unreacted Nb₃Sn superconducting composite wire. The superconductor wire used was removed from a Rutherford cable with the same dimensions as the dummy cable and 175 mm of excess length extends out of both sides of the blank and is bent at a 90° angle to form the current lead legs of the sample. The blank with the Nb₃Sn insert strand and the

* Corresponding author.

E-mail address: kovacs.34@osu.edu (C.J. Kovacs).

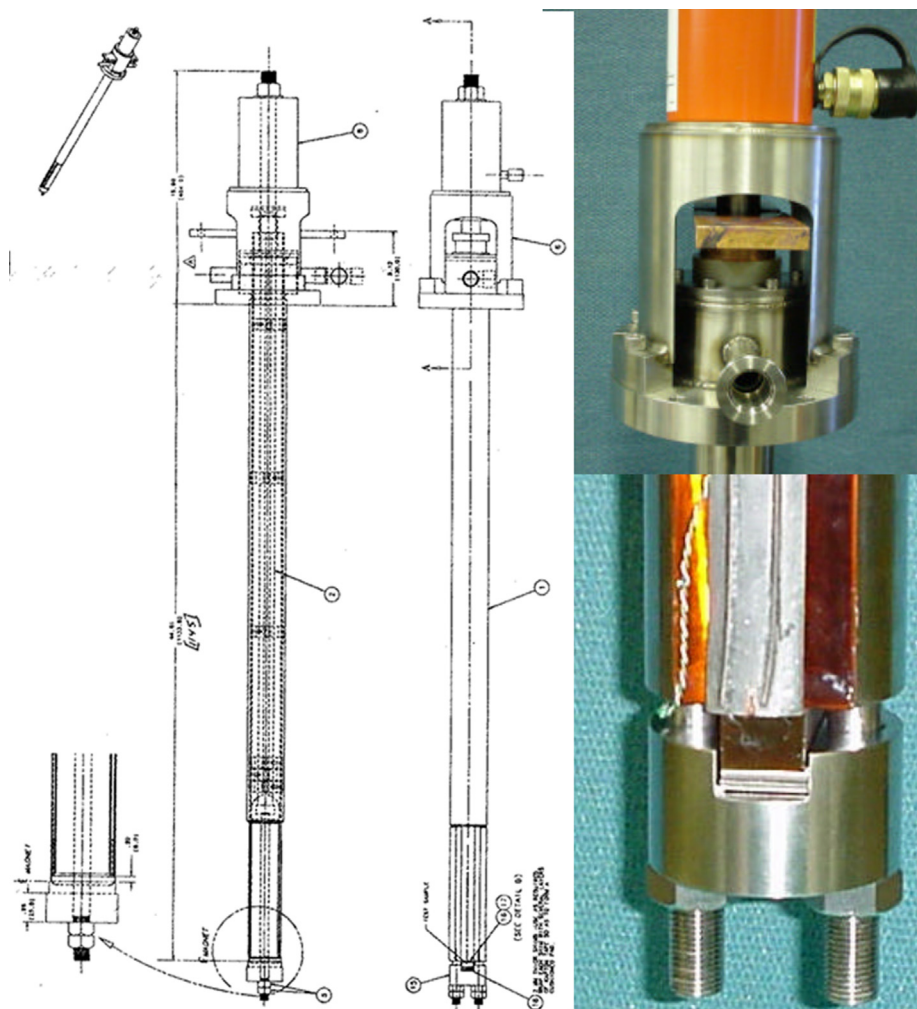


Fig. 1. The Fermilab transverse pressure insert, “TPI”, probe. (Left) Schematic of the entire TPI probe, (Top right) top of probe with the orange colored SPX Power Team® RH203 Model D hydraulic cylinder. (Bottom right) bottom of the pressing fixture, the sample shown is without Cu tabs or strand legs so the pressing bar is visible. (For interpretation of the references to colour in this figure legend, the reader is referred to the web version of this article.)

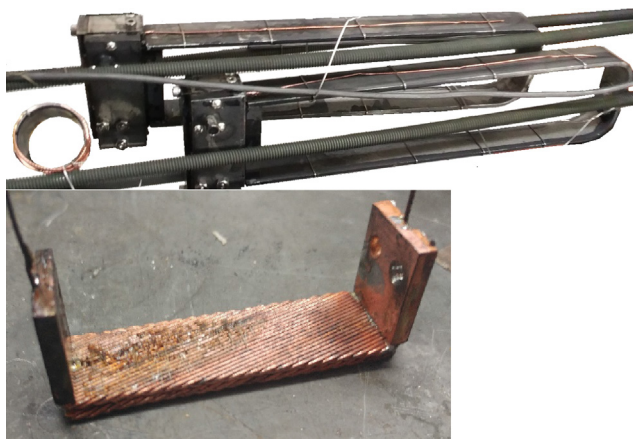


Fig. 2. (Top) TPI samples in reaction/impregnation fixtures getting loaded into a flowing Ar atmospherically controlled furnace. Shown in the bottom left of the image is one of the witness barrel samples. (Bottom) single Nb₃Sn strand embedded in the bottom dummy Rutherford cable blank of a two layer dummy cable blank stack. Soldered Cu tabs are shown; these are for increasing current carrying capacity near the bends and mechanical stabilization. The brown residue is from soldering flux and was removed before epoxy impregnation.

other blank were mounted onto a stainless steel or Inconel® 600 reaction/impregnation fixture and held in place with bolted plates and stainless steel wire; all of the bolts and contact surfaces were sprayed with dry graphite to prevent the bolts and plates from seizing. The loaded fixture were then placed in a flowing Ar furnace and heat treated, with witness barrel(s) and short straight samples, to form Nb₃Sn following a reaction heat treatment of 72 hr × 210C° → 48 hr × 400C° → 50 hr × 665 C° → furnace cool.

2.2. TPI sample fabrication: Preparing the sample for impregnation

After reaction, because the U-shaped sample was extremely delicate due to the small irreversible strain of reacted Nb₃Sn composite wires, care was taken during all handling steps. The steps before epoxy impregnation required opening the reaction fixture and handling the sample. The first handling step after reaction was soldering the ends of the blank stack. The Pb–Sn solder chosen had to be mechanically stable for subsequent sample preparation steps, including the temperatures of epoxy impregnation and curing. This soldering, introduced for mechanical and electrical stabilization of the sample, was performed near the Nb₃Sn wire’s 90-degree bends. Then, the stack was wound with S-glass tape with a 50% overlap. All the TPI sample fixture’s inner surfaces were sprayed with high temperature silicone release agent and the fixture was closed again. Two 8-inch lengths of R-3603 Tygon® tubing were attached to input and output ports of the fixture and the



Fig. 3. TPI sample vacuum impregnation fixture carrying two samples.

outer surfaces of the fixture were painted with a thin layer of Momentive® SS4004 primer. After this, the fixture was dipped in high temperature room temperature vulcanizing silicone (silicone RTV) to seal the gaps in the TPI sample fixture for vacuum epoxy impregnation. After silicone RTV drying, and vacuum testing of the seals, the fixture and sample were mounted onto a multi-unit simultaneous vacuum impregnation fixture and attached to evacuation ports and an impregnation manifold.

2.3. TPI sample fabrication: Vacuum epoxy impregnation

After silicone RTV drying, and vacuum testing of the seals, the fixture and samples were mounted onto a multi-unit simultaneous vacuum impregnation fixture and attached to evacuation ports and an impregnation manifold. See Fig. 3 for loaded and ready to impregnate TPI samples.

Degassed CTD-101 K vacuum impregnation occurred at room temperature, and after closing the evacuation ports, the epoxy was pre-cured at 110 °C for 5 h and then cured at 125 °C for 16 h.

NHMFL Mix-61 epoxy came in four components: Dibutyl Phthalate,

Aradur® 5200US, Tactix® 123, and Jeffamine® D 2000. The proper ratios of each component were weighed out (proprietary amounts) and each was preheated to 60 °C. Some of these components are viscous, and mixing was performed for 30 min at 60°C in an oven under a fume hood. After mixing, the epoxy mixture was degassed under ~ 1 Torr vacuum for 20 min. Vacuum impregnation of Mix-61 occurred at 60°C for ~ 1 h. After the one hour period the vacuum exhaust and inlets of all the sample fixtures were sealed, and a heat treatment at 60°C for 6 h was performed to ensure good impregnation. After this, a heat treatment of 100 °C for 24 h was performed to cure and harden the Mix-61.

2.4. Sample mounting onto the TPI

After epoxy curing, the samples were carefully removed from the fixtures. Gentle filing was performed to ensure smooth edges of the epoxy impregnated samples. A chosen sample would be mounted onto the TPI holder, the sample legs soldered to current leads, and the sample instrumented with two pairs of voltage taps. One pair of voltage taps was located 15 mm above the bottom face of the U-shaped sample, in the 90-degree bend. The other voltage tap pair was 80 mm up each current lead, soldered on top of the single Nb₃Sn strand.

The TPI probe, see Fig. 1, was commissioned in 2002 in a series of experiments investigating critical current (I_c) degradation of superconducting composites at 4.2 °K in the Teslatron II measurement station with applied fields of 14–16 T. The probe has current leads rated for up to 2000 A and has a SPX Power Team® RH203 Model D hydraulic cylinder capable of applying 20 Tons; the area conversion is up to ~250 MPa to the sample. The Enerpac® PEM Series 20 hydraulic pump lines had an analog hydraulic fluid pressure transducer to deliver an active signal of the fluid pressure and pressure onto the sample. This hydraulic fluid pressure signal does require a small correction to convert to pressure onto the sample due to deflections within the sample holder under high pressure. An Enerpac® V152 manually controlled valve was used to control pressure delivered to the sample.

For measurements performed in this document, a Pb-zirconate piezoelectric transducer behaving as an acoustic sensor was mounted onto the TPI pressing fixture. The acoustic sensor was within the sample pressing region (too short to be pressed by the fixture), and close to the side where the U-shaped sample was pressed (see Fig. 4). The pressure transducer signal (up to 5 V) was reduced with a resistor circuit. The reduced transducer signal, both pairs of voltage tap signals, and the acoustic sensor voltages were detected at 50 kHz using a NI-9238 module in a cRIO-9073 using 32-bit LabVIEW® 2018 in a 64-bit Windows® 10 operating system. All these measurements were simultaneously recorded using a National Instruments® SCXI-1327 card into a National Instruments® SCXI-1000 using a 32-bit LabVIEW® 2012 virtual instrument program (VI) on a computer running a 32-bit Windows® XP operating system. Because the NI-9238 measurements were

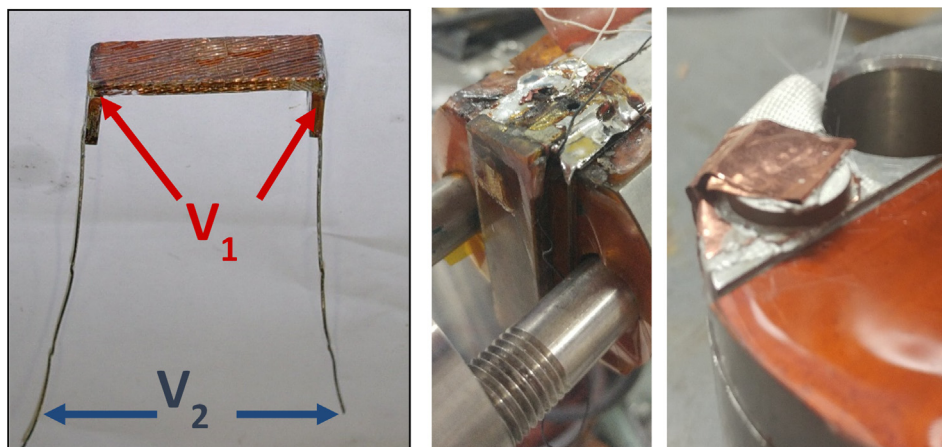


Fig. 4. TPI sample instrumentation. (Left) voltage tap pairs V_1 and V_2 . V_1 has a ~80 mm gauge length that measures the sample on both C tabs, right before entering the dummy Rutherford cable stack. V_2 taps are on the current leads with a ~180 mm gauge length. Only V_1 data was used for analysis and is shown in the results. (Middle) TPI sample mounted onto the probe. (Right) Acoustic sensor mounted on the pressing base near the sample. Cu foil tape was attached to the acoustic sensor using Ag epoxy.

Table 1

TPI sample 2, 3, and 4 measurement procedure.

- 13 T I_c measurement
- **1st Press:** 13 T i measurement with applying pressure, hold at each pressure for 20–60 s.
 - o 13.7 MPa “touchdown”
 - 41 MPa → 55 MPa → 68.5 MPa → 55 MPa → 41 MPa → 13.7 MPa
 - o systematic error of pressure $\begin{matrix} +6 \\ -3 \end{matrix}$ MPa
 - o ~16.5 MPa/min ramp-rate
- 13 T I_c measurement
- **2nd Press:** 13 T i measurement with applying pressure, hold at each pressure for 20–60 s.
 - o 13.7 MPa “touchdown”
 - 41 MPa → 55 MPa → 68.5 MPa → 55 MPa → 41 MPa → 13.7 MPa
 - o systematic error of pressure $\begin{matrix} +6 \\ -3 \end{matrix}$ MPa
 - o ~16.5 MPa/min ramp-rate
- 10 T I_c measurement
- **3rd Press:** 10 T i measurement with applying pressure, hold at each pressure for 20–60 s.
 - o 13.7 MPa “touchdown”
 - 41 MPa → 55 MPa → 68.5 MPa → 55 MPa → 41 MPa → 13.7 MPa
 - o systematic error of pressure $\begin{matrix} +6 \\ -3 \end{matrix}$ MPa
 - o ~16.5 MPa/min ramp-rate

Table 2

Sample specifications.

Sample#-press#-field (T)	Impregnation	Sample I_c , I_{press} , i (vs barrel)
S1-P1-13 T	CTD-101 K	350 A, 310 A, 0.78
S1-P2-10 T	CTD-101 K	563 A, 480 A, 0.68
S2-P1-13 T	CTD-101 K	49 A, 50 A, 0.13
S2-P2-13 T	CTD-101 K	—, 50 A, 0.13
S2-P3-10 T	CTD-101 K	101 A, 80 A, 0.11
S3-P1-13 T	NHMFL Mix-61	164 A, 140 A, 0.35
S3-P2-13 T	NHMFL Mix-61	—, 140 A, 0.35
S3-P3-10 T	NHMFL Mix-61	241 A, 220 A, 0.31
S4-P1-13 T	NHMFL Mix-61	249 A, 230 A, 0.58
S4-P2-13 T	NHMFL Mix-61	—, 230 A, 0.58
S4-P3-10 T	NHMFL Mix-61	422 A, 400 A, 0.56

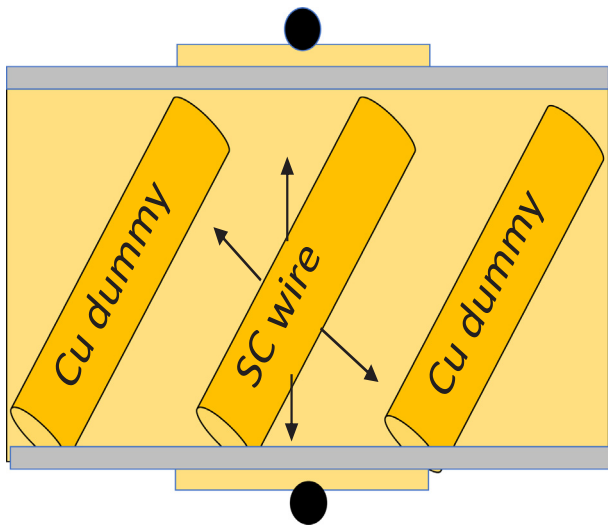


Fig. 5. Motion of the excitation current carrying superconducting strand within the transverse pressure insert sample. The voltage taps (black circles) are located on Cu tabs which, along with the excited strand and ends of the dummy cables, are soldered together. Assuming the dummy cables in this configuration behave as pickup coils in different orientations, and different strand motion displacement directions, it is possible to detect motion from the current carrying superconducting strand in the form of a voltage as described in Eq. (1).

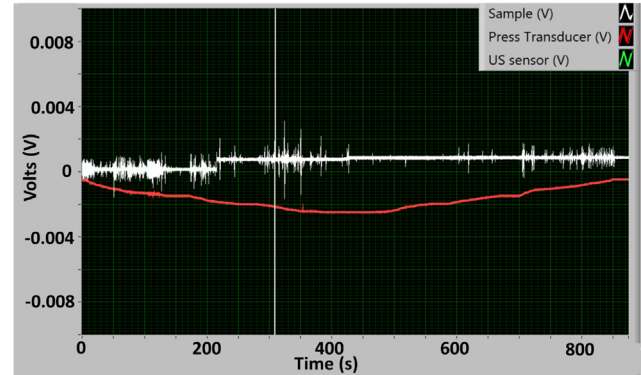
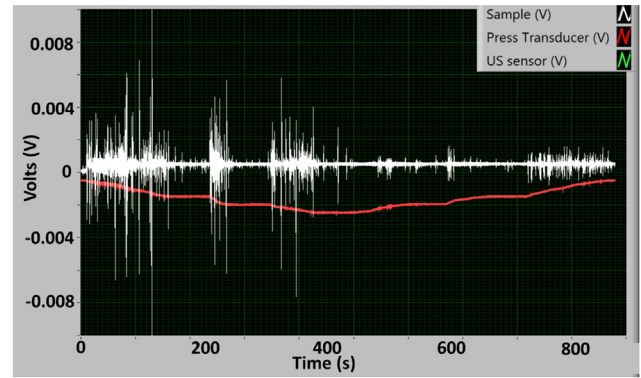


Fig. 6. (Top) voltage trace of S1-P1-13 T and (Bottom) voltage trace of S1-P2-10 T. The pressure dwell times were changed from longer ~60 s holds in S1-P1-13 T to ~20 s holds in S1-P2-10 T. A fixed jump in the baseline voltage was seen in both measurements, but was not seen in later measurements. There was no acoustic DAQ for this sample.

much more sensitive and with a faster acquisition rate, data from this data acquisition (DAQ) system was used to show results for pressing measurements while the SCXI 1327 data was used for the much slower I_c measurements. The procedure for samples 2–4 was as shown in Table 1.

The first sample followed the procedure in Table 1 except for the 2nd press and 2nd I_c measurement. Due to a different I_c (B) between samples, I/I_c (i) was calculated from the extracted cable strand I_c determined from witness barrel measurements.

3. Results

Four samples were prepared, two impregnated with CTD-101 K and two impregnated with NHMFL Mix-61. The first CTD-101 K sample measured only acquired the voltage tap signal during the pressure cycles and only had two pressing cycles versus three pressing cycles for samples 2–4. The I_c and i (calculated using the I_c from a witness barrel measurement) of each pressing measurement is shown in Table 2.

I_c was measured before the first 13 T measurement and before the 10 T measurement, except for the fourth sample which had 13 T I_c measured after the 10 T pressure experiment to check for possible degradation from pressing studies. Degradation of 8% was seen in the 13 T I_c after the three pressing cycles for the fourth sample. This may not be a surprise because the maximum transverse pressure of 68.5 MPa is close to the onset of I_c degradation seen in previous pressing studies of internal-tin Nb_3Sn Rutherford cable using this experimental system [8]. Because there was possible I_c degradation from each pressure cycle, in Table 2 the sample I_c is shown only for pressing measurements where I_c was measured before pressing. “ I_{press} ” is the transport current that was used during an entire pressing cycle.

From the data, it appeared the excited superconducting strand and

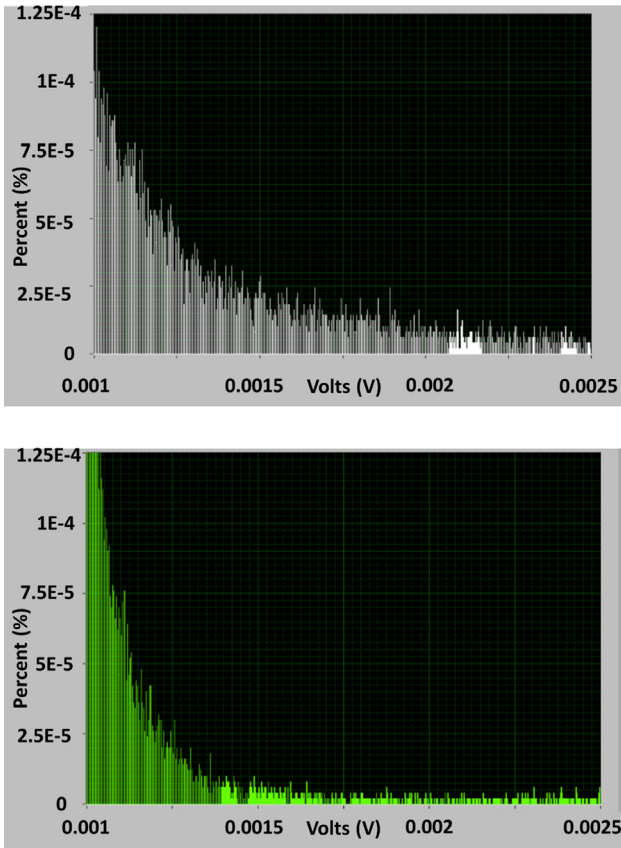


Fig. 7. (Top) Histogram data of the voltage trace of S1-P1-13 T and (Bottom) of the voltage trace of S1-P2-10 T. The histograms were symmetric around the same value near zero, and shown is the histogram data for voltage peaks with a positive sign outside of the noise spectrum. It is clear the first press for this sample, S1-P1-13 T, created a higher occurrence of high amplitude voltage peaks.

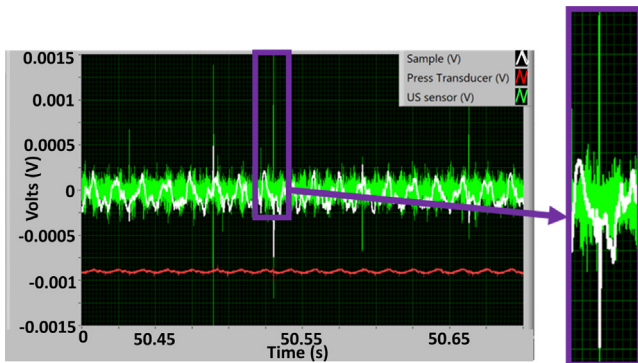


Fig. 8. A zoom in of the acoustic and voltage tap traces of S4-P1-13 T, wherever there is an acoustic peak (“US sensor”) there is an accompanying voltage peak that is above the noise floor. The peak matching shown in this figure is seen for all of the pressing data acquired for samples 2-4.

dummy cables functioned as an embedded and coupled magneto-mechanical inductive sensor that resolved motion of the excited strand. This is different from what was expected, a magnetothermalmechanical sensor that detects voltages from rapid normal zone transients [9]. A simplified diagram of the sample is shown in Fig. 5.

Assuming the excited strand axis is perpendicular to the normal of a single loop of the dummy cable stack outer dimensions and moves a small distance along the normal of the loop, it is possible to find expected voltages from reasonable input parameters (see Eq. (1)). In Eq.

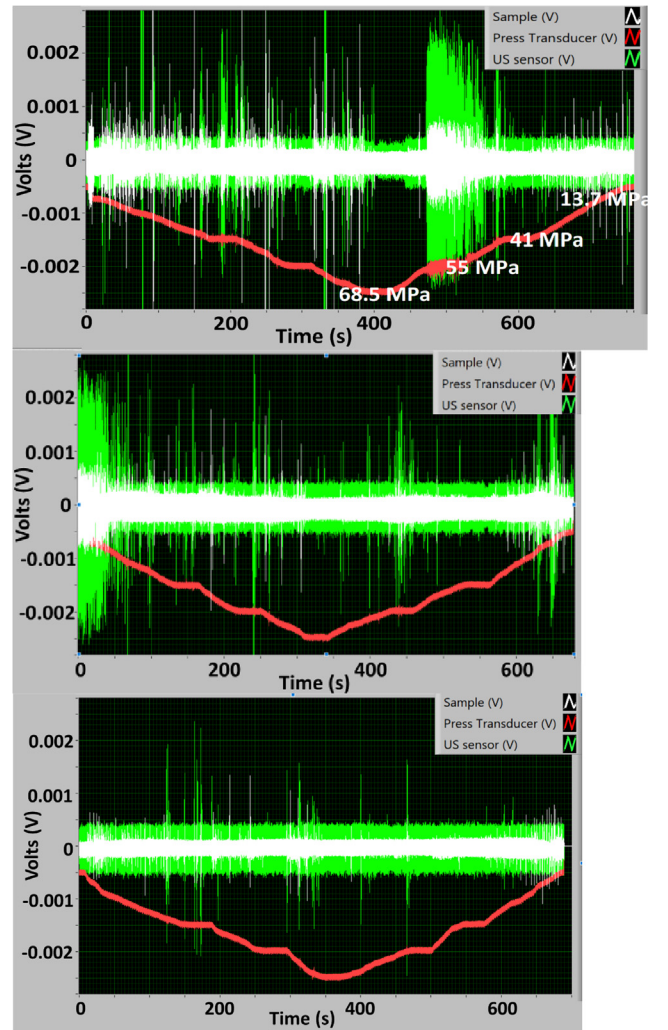


Fig. 9. Acoustic and v-tap data for (top down) S2-P1-13 T, S2-P2-13 T, and S2-P3-13 T.

(1), Φ is magnetic flux, t is time, I is current, μ_0 is the permeability of free space, r is radial distance, Δ “is change in”, and A_{loop} is area of the proposed inductive pickup loop.

$$\frac{d\Phi}{dt} = -\frac{\frac{dB}{dr} I}{\pi r^2} \times \frac{dr}{dt} \times A_{loop} \frac{dr}{dt} = 1 \frac{m}{s} \quad I = 500 \text{ A}$$

$$r = \frac{\text{cable width}}{2} = 0.007 \text{ m}$$

$$\rightarrow \quad (1)$$

$\Delta V = 255 \mu\text{V}$ to 2.9 mV (dependent on direction of strand motion)

This voltage value is a simple demonstration and will be dependent on: (i) the connectivity in the cable stack with soldered dummy cable ends, (ii) strand motion orientation, and (iii) the excitation of the current in the sample. Eq. (1) shows a linear relationship of voltage peak magnitudes and current in the excited strand. Because of this relationship, it was assumed there was a 1:1 linear relationship of the voltage peak magnitude with excited current and sample voltage tap data was normalized for cross comparison analysis.

3.1. Sample 1: First CTD-101 K sample

The I_c and measurement current of the sample at 13 T and 10 T were 350/310 A and 563/480 A respectively. Shown in Fig. 6 are the voltage signals that were recorded for the first two pressing cycles of the first

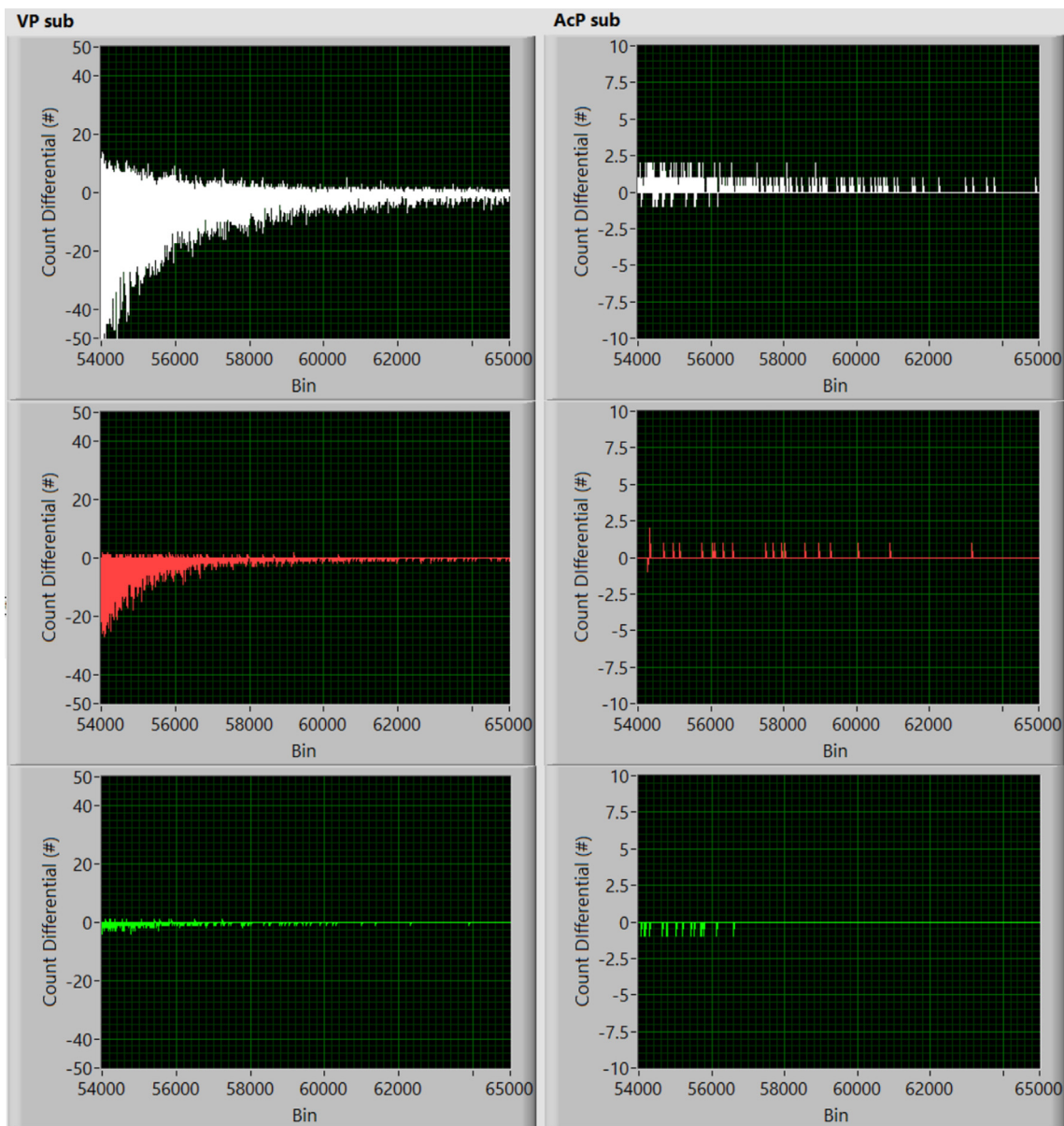


Fig. 10. Histogram differential of the fourth Mix 61 sample subtracted by the third Mix-61 sample; (top) press 1, (middle) press 2, and (bottom) press 3. Voltage tap data is in the left side of the figure and acoustic data is on the right.

CTD-101 K impregnated sample, no acoustic data was acquired. It is clear from this data, which had ~ 60 s dwell times, voltage peaks were generated mostly during pressure ramps. Additionally, the voltage data was plotted in a Histogram (100,000 bins, ± 0.0025 V) to show the first 13 T measurement had a higher frequency of higher amplitude peaks, see Fig. 7. The baseline jump seen in both data sets of Fig. 6 was not seen for other samples.

It must be mentioned that besides the amount of excitation current, the histogram relationships will also be altered by temporal differences in measurements including pressure ramp rates, time lengths of pressure holds in proportion to the entire data acquisition, and total time of the data acquisition. The same measurement procedure of the TPI samples 2–4 was attempted, but there are some small differences due to challenges in manually controlling the pressure using the Enerpac® PEM 20 series hydraulic pump and V152 control valve.

3.2. Sample 2: Second CTD-101 K sample

The I_c of the sample measured at 13 T and 10 T were 50 A and 80 A

respectively, a large reduction of I_c compared to the witness barrel measurement. Because smaller excitation currents reduced voltage signal amplitudes, the excitation current was set to I_c to maximize signal amplitude. This sample was the first with acoustic data acquisition and it became clear that both the voltage taps and the acoustic sensor response had excellent temporal matching, see Fig. 8. The polarity of the voltage and acoustic signals may have been different at times, but the occurrence of peaking occurred at the same time almost exclusively. This would support the reasoning that the magnet scale composite micro and macro fractures, detected acoustically, simultaneously generated strand motion.

The acoustic and voltage tap signatures of this second sample are shown for each pressing cycle in Fig. 9. Histograms of this data show the voltage tap data had a lower occurrence and lower magnitude of peaks for subsequent pressing cycles (this was seen for all four TPI samples). Histograms of this data also demonstrated the acoustic sensor data had a lower occurrence and lower magnitude of peaks with subsequent pressing cycles (same for TPI samples 3 and 4). This irreversible signal generation behavior is indicative of irreversible mechanical

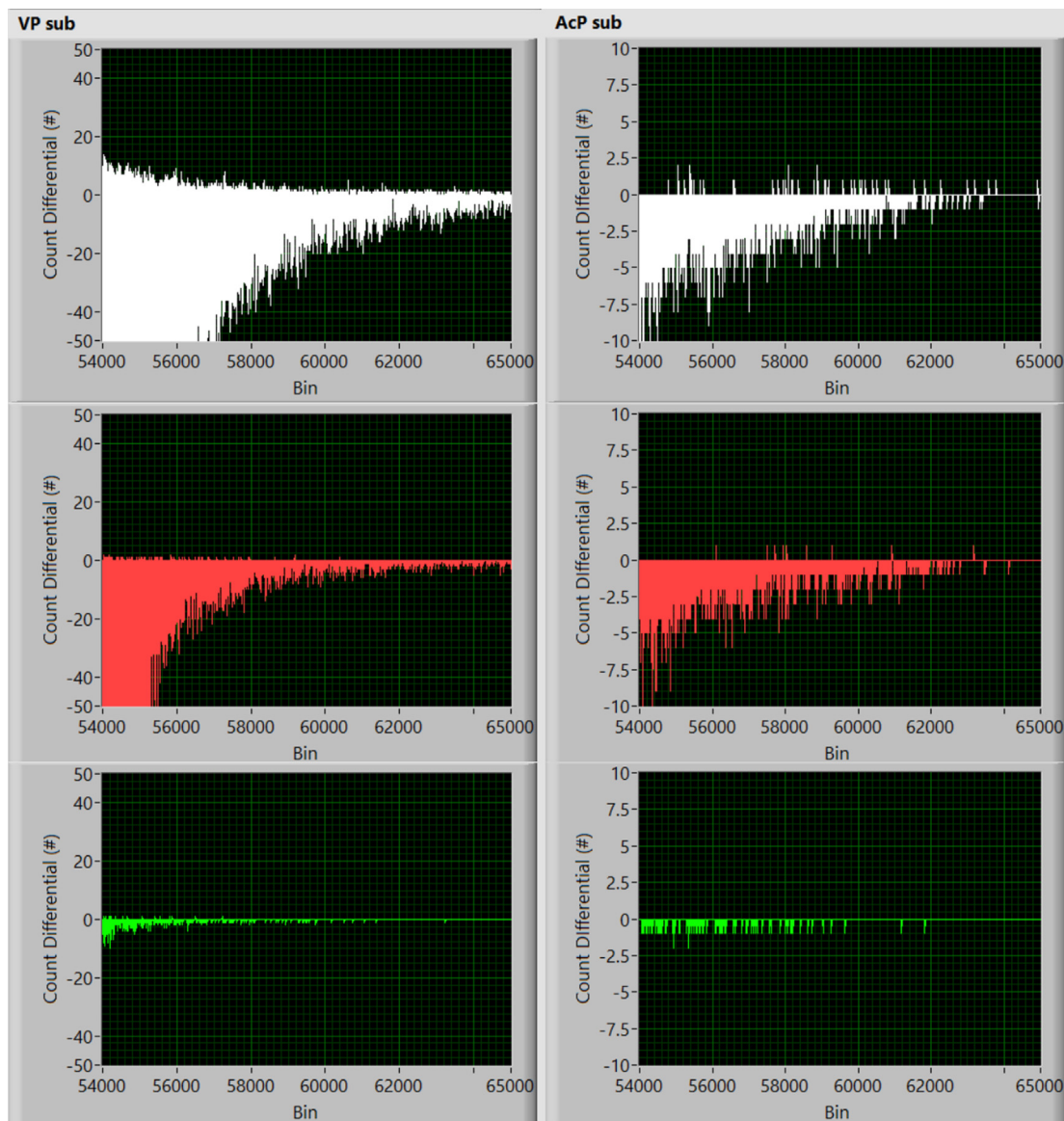


Fig. 11. Histogram differential of the fourth Mix-61 and the second CTD-101 K sample.

response, similar to what can be expected in cyclic loading during magnet ramping and training quench cycles.

3.3. Sample 3 and 4: First and second NHMFL Mix-61 samples

The I_c and measurement current of the third sample measured at 13 T and 10 T were 160/140 A and 239/220 A respectively, a reduction of I_c compared to the witness barrel measurement. The I_c and measurement current of the fourth sample (the second Mix-61 sample) at 13 T and 10 T were 249/230 A and 448/400 A respectively, near a 50% reduction in I_c compared to the witness barrel measurement. These two NHMFL Mix-61 samples demonstrated repeatability of these TPI measurements and accuracy of the current normalization used during analysis.

Shown in Fig. 10 are the subtraction of the first Mix-61 sample by the second Mix-61 sample histograms data of the normalized voltage tap and acoustic sensor signal. The voltage tap histogram for this analysis had 100000 bins from -0.0005 to 0.0005 V and the acoustic signal histogram had 100,000 bins from -0.01 to 0.01 V. This differential histogram data was symmetric over bin 50,000 and therefore in Fig. 10 the focus was to exclude redundant signals and those signals

similar in magnitude to the noise during the measurement. The bin 56,000 and 65,000 bounds in Fig. 10 for the excitation current normalized voltage tap data and acoustic data corresponds with 0.00004 – 0.00015 V and 0.0008 – 0.0030 V respectively.

With identical structure, processing, properties, an identical measurement procedure, and unchanged DAQ it should be expected that the acoustic signal histogram differential data should be near zero for each pressing cycle. This was indeed the case, and there was minimal difference between the acoustic signal histogram data for the fourth and third sample for all pressing cycles (the fourth sample had a slightly larger occurrence of high amplitude peaks). The voltage tap histograms of sample 3 and 4 should also have minimal histogram differential data, considering there was acoustic peak matching and assuming the normalization procedure of a linear correction was appropriate. The third sample had a slightly larger occurrence of high amplitude voltage tap peaks after normalization.

4. Discussion of the results

Because the fourth and third sample were similar, the fourth sample's (Mix-61) histograms were subtracted by the second sample's

(CTD–101 K). The same procedures for finding the differential between both Mix–61 samples (see Section 3.3) was used in the CTD–101 K/Mix–61 comparison. The differential histograms are shown in Fig. 11.

It is clear from this data that the CTD–101 K sample produced many more acoustic and voltage tap signals of larger magnitude (i.e. strand motion and structural damage). The differential histogram values are much smaller for the third pressing, but this is because the irreversible degradation has already been achieved. Assuming bulk magnet composite cracking (and not internal delamination and motion) is a leading cause for training in the high–field/lower pressure region of the next–generation of Nb₃Sn accelerator dipole magnets, this data suggests Mix–61 is a better impregnation material to reduce magnet training.

5. Summary

A sub–scale, single strand excitation measurement has been demonstrated to investigate acoustic generation and internal motions of accelerator magnet scale composite with applied transverse pressure cycles at 4.2 K in a transverse magnetic field. A magnet scale composite impregnated with CTD–101 K had more frequent high amplitude acoustic signals and strand motion versus a similar sample impregnated with NHMFL Mix–61 when going through a pressing cycle up to 68.5 MPa. It has been proposed in this document this system can rapidly investigate new impregnation materials and magnet scale composites to produce data relevant for predicting training behavior in Nb₃Sn accelerator magnets.

CRediT authorship contribution statement

C.J. Kovacs: Conceptualization, Methodology, Software, Validation, Investigation, Writing - original draft, Visualization. **E.Z. Barzi:** Conceptualization, Methodology, Investigation, Resources, Supervision, Project administration, Funding acquisition. **D. Turrioni:** Software, Investigation, Resources, Supervision. **A.V. Zlobin:** Conceptualization, Methodology, Resources, Supervision, Project administration, Funding acquisition. **M. Marchevsky:** Supervision.

Declaration of Competing Interest

The authors declare that they have no known competing financial interests or personal relationships that could have appeared to influence the work reported in this paper.

Acknowledgements

This work was supported by the United States Department of Energy, Office of Science, Division of High Energy Physics under grant: DE SC0011721. This work was also supported by Fermilab APS-TD and the United States Department of Energy, Office of Science, Science Graduate Student Research (SCGSR) program.

Appendix A. Supplementary material

Supplementary data to this article can be found online at <https://doi.org/10.1016/j.cryogenics.2019.103025>.

References

- [1] Gupta R, et al. Design, construction, and test of HTS/LTS hybrid dipole. *IEEE Trans Appl Supercon* 2018;28:3.
- [2] Schoerling D, Zlobin AV. Nb₃Sn accelerator magnets: designs, technologies, and performance. Springer Nature Switzerland AG; 2019.
- [3] Gourlay SA, et al. The U.S. magnet development program plan. Berkeley, CA, USA: U.S Magnet Development Program, LBNL; 2016.
- [4] A.V. Zlobin et al., Quench performance and field quality of the 15 T Nb₃Sn dipole demonstrator MDPCT1 in the first test run, Proceedings of NAPAC2019, Lansing, Michigan, Sept. 1–6 2019.
- [5] G. Velev et al., Fermilab superconducting Nb₃Sn high field magnet R&D program, 10th Int. Particle Accelerator Conf. (IPAC2019), Melbourne, Australia, May 19–24 2019.
- [6] Marchevsky M, Gourlay SA. Acoustic thermometry for detecting quenches in superconducting coils and conductor stacks. *Appl Phys Lett* 2017;110:012601.
- [7] Marchevsky M, et al. Axial-field magnetic quench antenna for the superconducting accelerator magnets. *IEEE Trans Appl Supercon* 2015;25:3.
- [8] E. Barzi and A.V. Zlobin, Superconductor requirements and characterization for high field accelerator magnets, 2015 IEEE I2MTC Proceedings, pp. 566–571 (2015).
- [9] Tsukamoto O, Maguire JF, Bobrov ES, Iwasa Y. Identification of quench origins in a superconductor with acoustic emission and voltage measurements. *Appl Phys Lett* 1981;39:2.